Applied Acoustics 161 (2020) 107163

Contents lists available at ScienceDirect

Applied Acoustics

journal homepage: www.elsevier.com/locate/apacoust

Chirp-rate quasi-orthogonality based DSSS-CDMA system for underwater acoustic channel

Fei Yuan *, Zhen-yu Jia, En Cheng

Key Laboratory of Underwater Acoustic Communication and Marine Information Technology (Xiamen University), Ministry of Education, Xiamen, China

ARTICLE INFO

Article history:
Received 23 March 2019
Accepted 21 November 2019

Keywords:
Underwater network node positioning
Chirp
DSSS-CDMA
Spread spectrum

ABSTRACT

Underwater network node positioning is a key supporting technology for underwater networks. Generally, nodes at known locations (anchor nodes) are used to transmit location information to the node to be located, and the node to be located performs location calculation according to the arrival time of the received information, which requires multiple access communication between the anchor nodes and the node to be located. In order to reduce the multiple access interference (MAI) and distinguish the information of different anchor nodes, it is necessary to study the underwater multiple access method. The GPS positioning system uses direct sequence spread spectrum code division multiple access(DSSS-CDMA) technology, and the positioning satellite transmits a signal formed by the BPSK modulation by transmitting a pseudo-random sequence (PN sequence) to the binary code sequence corresponding to the navigation message to the user equipment to be located. The underwater acoustic (UWA) channel has a complex multipath structure and Doppler effect, which causes a large interference to the communication system. Compared with narrowband communication, spread spectrum communication has a strong anti-interference ability, and can maintain the reliability of the communication system in the UWA channel. Based on this, this paper proposes a quasi-orthogonal Chirp-rate based DSSS-CDMA method under UWA channel, and carries out simulation analysis and experimental verification.

1. Introduction

Underwater node positioning is the key support technology of underwater network [1]. Generally speaking, the location information of multiple positioned nodes (anchor nodes) in the underwater network is often used to calculate the location information of other unlocated nodes. In order to correctly receive the location information from multiple anchor nodes to the unlocated nodes, underwater multiple access (MA) has become a very important supporting technology in the positioning system [2].

Underwater acoustic (UWA) channels are one of the most complex channels on earth. They can be equivalent to a complex time-variant, space-variant and frequency-variant filter [3], The signals will be severely distorted when it reaches the receiver through the UWA channel, which is an important factor affecting the effectiveness and reliability of the UWA communication system. The spread spectrum is considered as one of the most effective techniques for conquering fading and jamming channels, such as the underwater acoustic channel, among others. It can improve the reliability of the communication system and is an optimal choice for an UWA channel [4].

In the Global Positioning System (GPS), the positioning satellites first use PN sequences to spread the spectrum of the data to be transmitted, and then use BPSK modulation to transmit the information to the receiver. To obtain the positioning information correctly, the PN sequences and carriers at the receiver must be the same with the transmitter [5]. This method is direct spread spectrum code division multiple access scheme (DSSS-CDMA), which uses the orthogonal PN sequences to carry bit data to build up a M-ary spread spectrum system. In [6], the M-ary spread spectrum is performed by PN sequences to improve the spectrum efficiency. In [7], a higher data rate spread spectrum system based on orthogonal sequences was designed. In [8], passive time reversal DSSS underwater communication was investigated to achieve further performance enhancement via the multipath temporal-spatial focusing. Additionally, in [9], a UWA communication system based on M-ary bionic signal coding was proposed for high spread spectrum gain.

DSSS-CDMA uses PN code for spread spectrum, which is susceptible to the multipath and Doppler effect in the UWA channel. Chirp signal is a pulse compression signal with its own spread

* Corresponding author.
E-mail address: yuanfei@xmu.edu.cn (F. Yuan).

https://doi.org/10.1016/j.apacoust.2019.107163
0003-682X/

spectrum properties. It has good anti-noise, anti-multipath and anti-Doppler performances [10], so it is widely used in the field of UWA communication. During its duration, the frequency of the signal changes linearly with time. According to the linear increase or decrease of the frequency, it can be divided into Up-Chirp and Down-Chirp signals. Wang et al. [11] analysed the performance of the Chirp-BOK (Binary Orthogonal Keying) modulation method.

Cook et al. [12] proposed a multiple access method based on Chirp signals for the first time, each user is assigned a pair of Chirp signals (Up-Chirp and Down-Chirp), users are distinguished by different Chirp-rates and bandwidth, and the orthogonality of the Chirp signals can effectively suppress multiple access interference (MAI). However, in a limited bandwidth, as the number of users increases, the MAI also increases, resulting in a decrease in performance. Hengstler et al. [13] proposed an improved method to assign a specific Chirp-rate and an initial phase to each user. This method uses Chirp-rates to distinguish the users, and different initial phases are used to guarantee the orthogonality of users. Although this method reduces the MAI to some extent, it also reduces the channel capacity. Ju and Barkat [14] proposed a bandwidth-overlapping modulation method, and it reduces MAI by using an orthogonal Chirp signals group, which is similar to OFDM. The experimental results showed that the technology can easily handle a larger number of users than the method in [12]. However, in the UWA channel, the available bandwidth is very limited, and the multipath effect is also very serious. In above methods, as the number of users increases, the bandwidth of each user's Chirp signal decreases, resulting in more serious MAI, and the bit error rate (BER) performance get worse. To solve this problem, Meng and Gu [15] proposed a combined Chirp signal with different Chirp-rate, and then assign these quasi-orthogonal signals to users, which greatly improved the BER performance of the system. Sha et al. [16] proposed a new multiple access method that uses the width of the band to distinguish users. This method processes signals in the Fractional Fourier Transform (FrFT) domain to avoid high synchronization requirements in multiple access systems.

With the development of new technologies, the multiple access method based on Chirp signal tends to be combined with other methods, which can further suppress the MAI. Kocian and Dahlhaus [17] proposed a method combining Chirp carriers and DSSS-CDMA in the field of wireless communication. The method uses the quasi-orthogonality between different Chirp signals to suppress the MAI, and replaces the PN code with the Up-Chirp and Down-Chirp signals. The bandwidth occupied by the system is determined by the Chirp signals, not the PN sequences. El-Khamy et al. [18] proposed a modulation method of Chirp signals based on broadband time-varying, which is used in frequency hopping code division multiple access (FH-CDMA) system. Gupta et al. [19] proposed a method combining Chirp signal and fast FH-CDMA in the field of wireless communication, which greatly improves the BER performance, but it also leads to the problem of low bandwidth efficiency. Peng et al. [20] further proposed a modulation scheme combining OFDM and Chirp signal. By using Chirp signals with better orthogonality in the subchannels of OFDM for modulation, interference due to frequency deviation between subchannels can be eliminated.

The paper is organized as follows. Section 2 introduces the basic principles of DSSS-CDMA firstly, then introduces the modulation method of Chirp-BOK, and finally introduces the FrFT for a faster demodulation and users separation method. In Section 3, a DSSS-CDMA system based on Chirp-rate quasi-orthogonality is proposed, and the sender and receiver are introduced in detail. Section 4 analyses the anti-noise and anti-multipath performance of the proposed system based on the characteristics of Chirp signals in the FrFT domain. Section 5 presents the performance analysis about the proposed method in the UWA channel, and then verifies it through simulation and experimental data. Section 6 completes the paper with concluding remarks.

2. Principle and derivation

This section first introduces the basic principle of DSSS-CDMA, and then introduces the Chirp-BOK modulation. Finally, for a faster demodulation method, Fractional Fourier Transform (FrFT) is introduced.

2.1. DSSS-CDMA

In the DSSS-CDMA system, the user's data is spread by a PN sequence, then modulated onto a single frequency carrier and sent to the channel [21]. The chip width of each code of the PN sequence is much smaller than the width of one bit data. Therefore, the chip rate is much higher than the bit rate, as a result, the spectrum of the signal is spread.

DSSS-CDMA system allocates mutually orthogonal PN sequences to users, and each user spreads its own data using its own PN sequence. At the receiver, the received signal is despread by the same PN sequences, and then demodulated by the corresponding carrier, finally the data sent by different users [21] can be obtained.

The signal sent by mth user is given by:

$$b_m(t) = \sum_{k=0}^{\infty} b_m(k) g(t - kT), b(k) = \pm 1, \tag{1}$$

where T represents the chip width of the bit data, $b_m(k)$ is the bit data stream, and $g(t - kT)$ is a rectangular pulse of duration T. Let $\rho_m(t)$ be the mth user's PN sequence signal, and it's given by:

$$\rho_m(t) = \sum_{n=1}^{N} \rho_m^n g(t - nT_{pn}), \rho_m^n = \pm 1, \tag{2}$$

where T_{pn} is the chip width of PN code, and T is N times T_{pn}. Let $s_m(t)$ be the transmitter signal of the mth user. And the $s_m(t)$ is given by:

$$\begin{aligned} s_m(t) &= b_m(t)\rho(t)\cos w_0 t \\ &= \sum_{k=1}^{\infty} b_m(k) \cdot \left[\sum_{n=1}^{N} \rho_m^n g(t - nT_{pn}) \right] \cdot \cos w_0 t. \end{aligned} \tag{3}$$

Let the $\beta(t)$ be the interference from other users, $n(t)$ be the noise signal. The received signal $r(t)$ is given by:

$$r(t) = s_m(t) + \beta(t) + n(t), \tag{4}$$

The received signal is firstly despread by the same PN sequence signal $\rho_m(t)$. Let the despread signal be $d'(t)$, which is given by:

$$d'(t) = r(t)\rho(t) = s_m(t)\rho(t) + \beta(t)\rho(t) + n(t)\rho(t), \tag{5}$$

where

$$s_m(t)\rho(t) = b_m(t)\rho(t)\rho(t)\cos w_0 t = b_m(t)\cos w_0 t. \tag{6}$$

Finally, BPSK demodulation is performed to obtain the mth user's data. Due to the orthogonality between the PN sequences, after despreading, the interference signals of other users are effectively suppressed, and the spectrum of the noise signal is spread, correspondingly, the spectral density is reduced, so that the noise interference is reduced.

2.2. Chirp binary orthogonal keying (BOK) modulation

The expression of the Up-Chirp and Down-Chirp signals are given by:

$$S_{up}(t) = \cos\left(2\pi f_0 t + k\pi t^2\right), 0 < t < T \tag{7}$$

$$S_{down}(t) = \cos\left(2\pi(f_0 + kT)t - k\pi t^2\right), 0 < t < T \tag{8}$$

where f_0 represents the center frequency and T is the duration of the signal, k is the Chirp-rate of the Up-Chirp signal, and $-k$ is the Chirp-rate of the Down-Chirp signal, where k is a positive integer.

Based on the orthogonality of the Up-Chirp and Down-Chirp signals, the Chirp-BOK system uses a group of Chirp signals to modulate. The bit data is used to key up and down the Chirp signal. At the receiver, the matched filters of the Up-Chirp and Down-Chirp signals are used to finally obtain the transmitted data. The Up-Chirp and Down-Chirp is shown in Fig. 1: At the receiver, the received signal respectively enters the branches of the Up-Chirp and Down-Chirp matched filters. Fig. 2 shows the output of the two matched filters output when receiving the Up-Chirp signal:

Since the output waveform of the matched filter of the upper branch has a peak value, it can be judged that the received signal is an Up-Chirp signal, and then the received data is judged.

2.3. Fractional Fourier transform

Fractional Fourier Transform (FrFT) [22] is an outstanding S-T method in dealing with the LFM-like signals. It focuses the power in the FrFT domain [23,11] and does not introduce cross-interference. As an extension of the Fourier Transform, FrFT also possesses a fast calculation which reduces the computational complexity and makes it suitable for LFM-like signals detection. The FrFT of the received signal $x(t)$ can be expressed as:

$$X_p(u) = \int_{-\infty}^{+\infty} K_p(t,u)x(t)dt, \tag{9}$$

The $K_p(t,u)$ is expressed as:

$$K_p(t,u) = \begin{cases} A_\alpha \exp\left[j\pi\left(u^2\cot\alpha - 2ut\csc\alpha + t^2\cot\alpha\right)\right] & \alpha \neq n\pi \\ \delta(t-u) & \alpha = 2n\pi \\ \delta(t+u) & \alpha = (2n\pm 1)\pi \end{cases} \tag{10}$$

where the coefficient $A_\alpha = \sqrt{1 - j\cot\alpha}$, the transformation angle $\alpha = p\pi/2$, the order $p \neq 2n$, and n is an integer.

The traditional computation of the FrFT is complicated compared to the Fast Fourier Transform (FFT). Simplified FrFT algorithm proposed by Chen [24] help to reduce the complexity significantly, which is given by:

$$X_\alpha(f') = \int_{-\infty}^{+\infty} \exp\left[j(\pi\cot\alpha)t^2 - j2\pi f' t\right]x(t)dt, \alpha \in (0,\pi), \tag{11}$$

The discrete form of it can be expressed as:

$$X_\alpha(k) = \sum_{n=0}^{N-1} x\left(\frac{n}{\sqrt{N}}\right)\exp\left[j(\pi\cot\alpha)\left(\frac{n}{\sqrt{N}}\right)^2 - j\frac{2\pi}{N}nk\right], \tag{12}$$

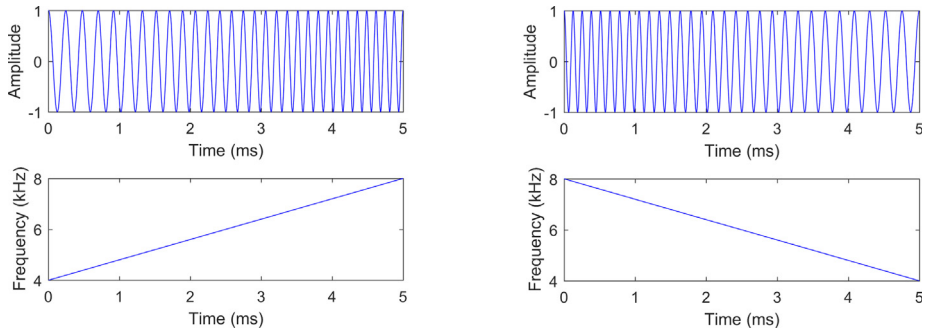

(a) Up-Chirp signal. (b) Down-Chirp signal.

Fig. 1. Waveform and time-frequency relationship of Chirp signals.

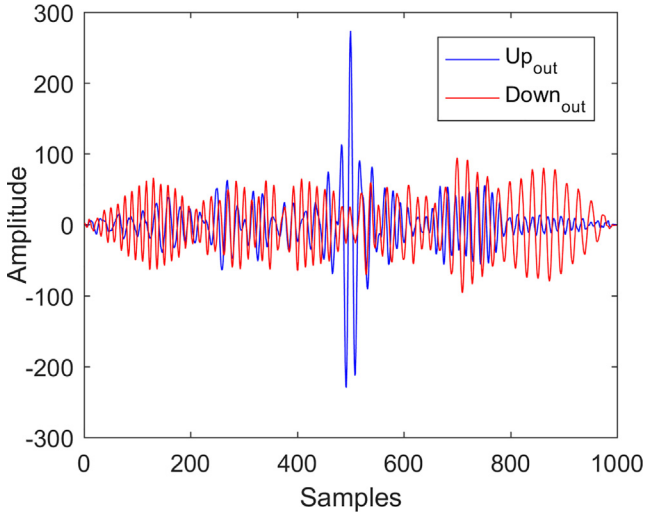

Fig. 2. Output of the matched filter.

where N is the number of sampling points. For a Chirp signal, it's optimal order p for FrFT is given by:

$$p = \frac{2\text{arccot}(f_s/B)}{\pi} + 1, \tag{13}$$

where f_s is the sampling rate of the system. It can be seen from Eq. (13) that in a communication system with a fixed sampling frequency f_s, the optimal FrFT transform order of the Chirp signal is determined only by the bandwidth it occupies. Under the premise that the chip width of the Chirp signal is the same, the optimal order is determined only by the Chirp-rate of the signal. When p is the optimal order, the Chirp signal focus the power in the FrFT domain, which is shown in Fig. 3.

3. Chirp-rate based DSSS-CDMA system

In a multiple access system based on Chirp-rate quasi-orthogonality, when the number of users increases, the Chirp-rate difference is compressed, leading to the increase of MAI. Moreover, the actual bandwidth occupied by users with lower Chirp-rates also get smaller. In the UWA channel, since the frequency selective fading is more serious, the decreasing of BT_c reduces the detection performance of Chirp-BOK communication system [25]. In this section, a Chirp-rate based DSSS-CDMA system is proposed by assigning mutually orthogonal PN sequences to different users and then using quasi-orthogonal Chirp signals for modulation. This method enhances the orthogonality between users, fur-

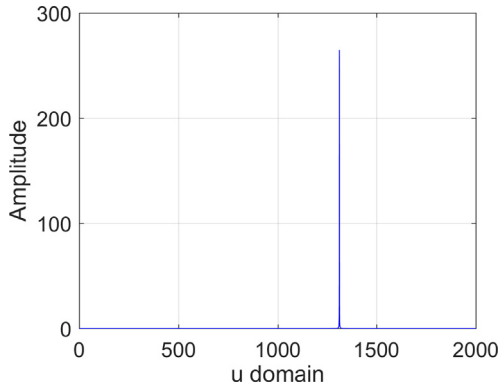

Fig. 3. The optimal order FRFT domain of Chirp signal.

ther suppresses MAI, and improves the reliability of multi-node communication in the underwater node positioning system.

3.1. System framework

Fig. 4 shows the framework of the Chirp-rate based DSSS-CDMA communication system. At the transmitter, the users' bit data are firstly spread by PN sequences, and the spread data are BOK modulated by users' carriers of different Chirp-rates, then the signals pass through the D/A converter, the power amplifier and the transducer, and finally transmitted to the UWA channel. After receiving the signal, the receiver firstly captures and preprocesses the signal. And then demodulates the signal using the FrFT of different optimal orders according to the Chirp-rates of different users, and then despreads the data using PN sequences, and finally obtains the users' transmitted bit data.

The part in the dashed box on the top of Fig. 4 shows the frame structure of the signal. A signal frame contains a synchronization header, a pilot signal for channel estimation, a piece of communication signal, and two guard periods (GP). The portion of each dashed box represents a module of the system. In the "synchronization and pre-processing" module, the pre-processing includes the channel estimation and the processing by the virtual time reversal mirror (VTRM), and it is used to obtain useful signals of each user.

3.2. Transmitter

Let the bit data sent by the mth user at a certain moment be $b_m(b_m \in \{0,1\})$, and the chip width is T. Due to the modulation method of BOK, it is converted into bipolar data, and $b_m \in \{-1,1\}$. The PN sequence of length N assigned to the mth user ρ_m is used to spread the data. Assuming that the chip width of each PN code is T_{pn}, and its relationship with T is:

$$T_{pn} = T/N. \tag{14}$$

After spreaded by the PN sequence, the data become $b_m\rho_m^n, n \in [1,N]$. And then the spread data is modulated onto the Chirp carrier using Chirp-BOK. The signal sent by mth the user is given by:

$$C_m(t) = \sum_{n=1}^{N}\left[\cos\left(2\pi\left(f_0 - \frac{b_m\rho_m^n - 1}{2}k_m T_{pn}\right)(t - nT_{pn}) + b_m\rho_m^n k_m \pi(t - nT_{pn})^2\right)\cdot g(t - nT_{pn})\right], \tag{15}$$

where k_m is the Chirp-rate of the Up-Chirp signal of the mth user. It can be seen from Eq. (15) that the Chirp-rate of the transmitted signal of the mth user is keyed by the spread data, and the duration of the Chirp signal is equal to the chip width of PN code. After Chirp-BOK modulation, N end-to-end Chirp signals are formed to transmit the bit data, the data transmission rate is determined by the chip width of the PN code. Fig. 5 shows the time-frequency relationship of the transmitted signal of the mth user:

3.2.1. Chirp carriers selection

The time-frequency relationship of the Chirp carriers of different users is shown in Fig. 6. As can be seen, different users correspond to different Chirp-rates. Due to Chirp-BOK modulation, each user's assigned carriers includes an Up-Chirp and a Down-Chirp. The Chirp carriers used by different users have the same chip width and centre frequency. Different Chirp-rates maintain

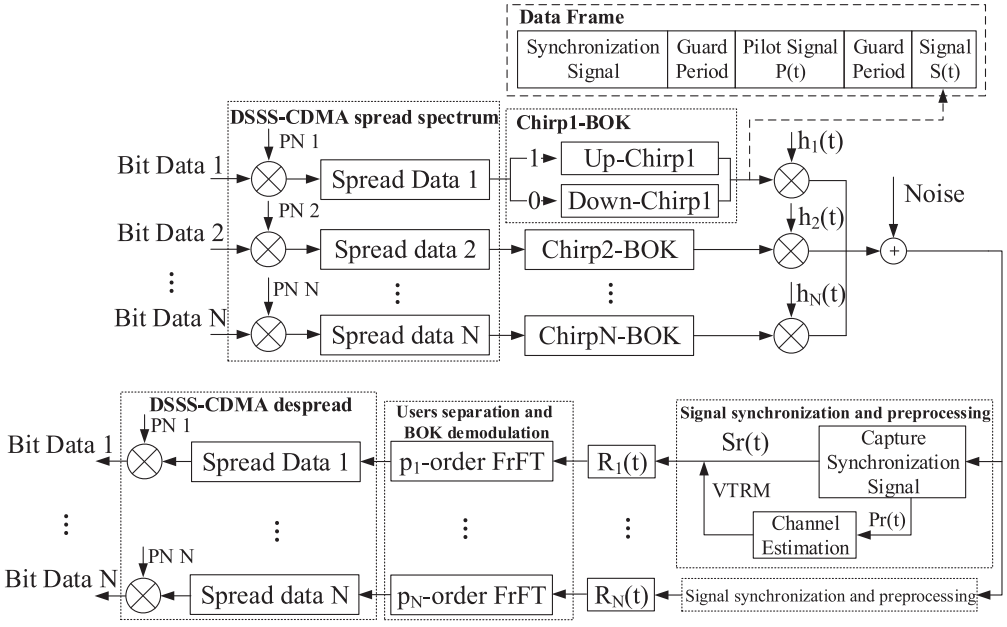

Fig. 4. Communication system principle framework.

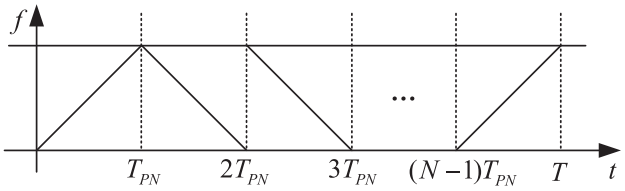

Fig. 5. The time-frequency relationship of the modulated signal.

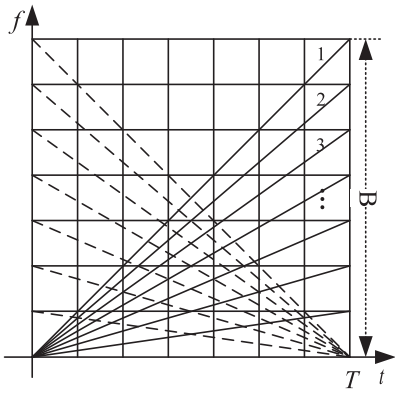

Fig. 6. Time-frequency relationship of users' Chirp carriers.

the quasi-orthogonality between the users' carriers, and suppress the MAI.

Under the AWGN channel, the bit error rate (BER) of the Chirp-BOK system is given by [11]:

$$P_f(\rho,\gamma) = Q(a,b) - \frac{1}{2}\exp\left(\frac{-\left(a^2+b^2\right)}{2}\right) I_0(ab), \tag{16}$$

where $Q(x)$ is Q function, γ represents the SNR (Eb/N0) of the received signal, $I_0(ab)$ is the zero-order Bessel function, and the a and b are given by:

$$a = \sqrt{\frac{\gamma}{2}\left(1-\sqrt{1-|\rho|^2}\right)}, \quad b = \sqrt{\frac{\gamma}{2}\left(1-\sqrt{1+|\rho|^2}\right)}, \tag{17}$$

and

$$|\rho| = \frac{1}{\sqrt{BT}}\sqrt{\left(C\left(\frac{\pi}{2}BT_c\right)\right)^2 + \left(S\left(\frac{\pi}{2}BT_c\right)\right)^2}. \tag{18}$$

From Eq. (18), we can see that the larger the BT_c, the smaller the $|\rho|$, which results in a smaller false detection probability. Thus, the increasing of BT_c improves the detection performance [25]. Fig. 7 illustrates the BER performance under different $|\rho|$ according to the Eq. (16), we can see that when the $|\rho|$ gets smaller, the BER performance of the Chirp-BOK system gets better.

In order to suppress MAI as much as possible, it is necessary to keep them orthogonal by reasonably controlling the Chirp-rate of different user carriers.

The Up-Chirp signal of each user is given by:

$$S_m(t) = \cos\left(2\pi f_0 t + k_m \pi t^2\right), m = 1,2,\cdots,M. \tag{19}$$

Let the correlations between the lth and mth Chirp carriers be $\rho_{l,m}$:

$$\rho_{l,m} = \frac{1}{E}\int_0^T S_l^*(t) S_m(t) dt, \tag{20}$$

where $S_l(t)$ and $S_m(t)$ represent two carriers numbered l and m in the Fig. 6, respectively, and E represents signal energy. Let the

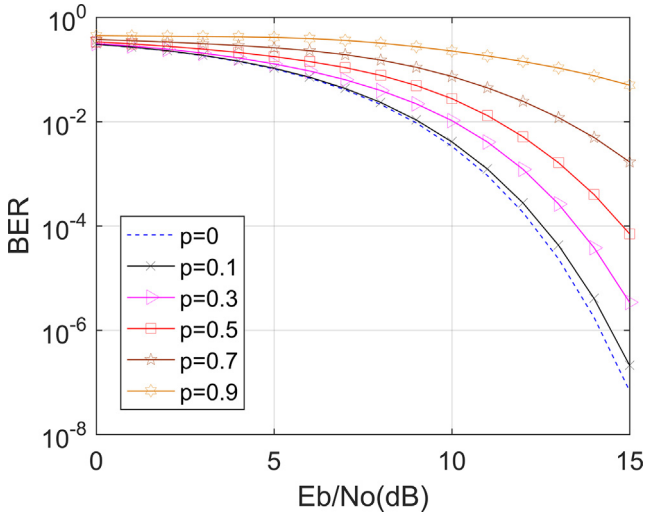

Fig. 7. Relation between ρ and BER performance.

amplitude A of the signal be $\sqrt{2E/T}$. According to Eq. (19) and (20):

$$\begin{aligned}\rho_{l,m} &= \tfrac{1}{T}\int_0^T \cos\left(2\pi f_0 t + \pi k_m t^2\right)\cos\left(2\pi f_0 t + \pi k_l t^2\right) dt \\ &= \tfrac{1}{T}\int_0^T \left[\cos\left(\pi(k_m - k_l)t^2\right) + \cos\left(4\pi f_0 t + \pi(k_l + k_m)t^2\right)\right] dt.\end{aligned} \tag{21}$$

Ignoring the high frequency integral term, Eq. (21) can be simplified to:

$$\rho_{l,m} = \frac{1}{T}\int_0^T \cos\left(\pi(k_m - k_l)t^2\right) dt. \tag{22}$$

Define the Chirp-rate difference between two signals as Δk, and

$$\Delta k = k_m - k_l, \tag{23}$$

$$\rho_{l,m} = \frac{1}{T}\int_0^T \cos\left(\pi \Delta k t^2\right) dt. \tag{24}$$

It can be seen from Eq. (24) that $\rho_{l,m}$ is a function of Δk and the chip width T. In a limited frequency band, Chirp-rate is determined by the total bandwidth B occupied by the system and the chip width, which indicates that the value of $\rho_{l,m}$ is related with the value of the time-bandwidth product BT and the difference of the Chirp-rate Δk.

Fig. 8(a) shows the relationship between $\rho_{l,m}$ and BT. The Chirp-rate of the two signals are 1000 kHz/s and 500 kHz/s, respectively. When Δk remains unchanged, $\rho_{l,m}$ and BT are generally negatively correlated. As can be seen, when the BT is greater than 100, $\rho_{l,m}$ gradually approaches 0, and we can say that the two signals are quasi-orthogonal. However, there is often not so much time and bandwidth resources available in the UWA channel, so other parameters need to be controlled to reduce $\rho_{l,m}$.

Fig. 8(b) shows the relationship between $\rho_{l,m}$ and the Δk between the two Chirp signals, where the bandwidth B is 10 kHz, and the chip width of the Chirp signal is 10 ms. The time-bandwidth product BT resources occupied by the system is 100. We can see that $\rho_{l,m}$ and Δk are generally negatively correlated, and it has also oscillated repeatedly and periodically appears to have a minimum value, which means that when the number of users is small, the quasi-orthogonality between carriers can be maintained by increasing the Δk as much as possible, and when the number of users is relatively large, an appropriate Δk can be selected according to Fig. 8(b) to ensure that $\rho_{l,m}$ is in a lower range, thereby ensuring the reliability of the system.

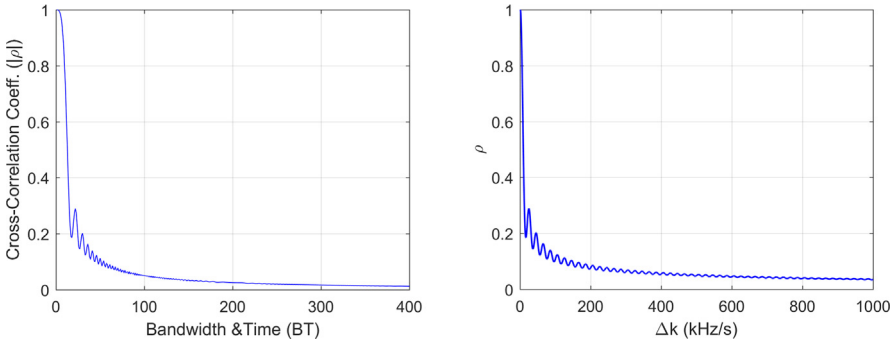

(a) Relation between BT and ρ. (b) Relation between Δk and ρ.

Fig. 8. Relation between ρ and the Chirp signals' parameters.

In the UWA channel, the range of available bandwidth is very limited. In the medium and short range communication to which underwater node positioning is applied, the available frequency band range is on the order of 10 kHz. Here, a frequency band of 20;kHz–30 kHz is used, In order to ensure that the system can occupy enough *BT*, the Chirp signal chip width is set to 10 ms.

In a multiple access system, when the number of access users is sufficient, we can make the expected BER performance of each user equal to the average BER of the whole system, so that the whole system has a good performance. Through the equal difference distribution of Chirp-rate, the same cross-correlation is maintained between the signals, so that the expected communication quality of each user is the same.

3.2.2. PN sequence selection

The PN sequence should first have sharp autocorrelation properties, which ensure that the signal after despreading have a higher SNR. Moreover, in order to reduce MAI, the cross-correlation coefficient of the PN sequences should also be as small as possible, which can effectively enhance the orthogonality between users. The Gold sequences are used in GPS [5], The GPS C/A ranging codes are Gold sequence of period 1,023. Since the Gold sequence is generated from a sequence with better cross-correlation in the m sequence, the number of correlations between the generated Gold sequences does not exceed the original m sequence preferably has a cross-correlation coefficient and therefore has excellent cross-correlation properties [26]. Preferably, a zero is added to the end of the generated Gold sequence, to generate an orthogonal Gold sequence. Orthogonal Gold sequences have both good autocorrelation properties and cross-correlation properties.

Fig. 9a and b show the cross-correlation properties of the m sequence and orthogonal Gold sequence respectively. As can be seen, the Gold sequences have better cross-correlation properties, which means that the DSSS-CDMA systems using Gold sequences have lower MAI.

In order to balance the bit rate and MAI suppression, an 8-bit orthogonal Gold sequence is used here. The chip width of the PN sequence is the same as Chirp signal, which is 10 ms.

3.3. Receiver

3.3.1. Channel estimation by chirp singal in FrFT domain

Assuming that transmit pilot signal for channel estimation is $x(t)$, and $n(t)$ is the noise signal, and channel impulse response can be written as follow:

$$h(t) = A_0\delta(t) + \sum_{i=1}^{L-1} A_i\delta(t - t_i), \tag{25}$$

where L represents the number of multipaths, A_i and T_i represent the magnitude and time delay of the ith path, respectively.

After the FRFT operation, receiving signal can be expressed as:

$$R_p(u) = A_0X_p(u) + \sum_{i=1}^{L-1} A_iX_p(u - \tau_i\cos\alpha)\exp\left[j\pi\left(\tau_i^2\sin\alpha\cos\alpha - 2u\tau_i\sin\alpha\right)\right] + N_p(u). \tag{26}$$

From Eq. (26) we can see that different delay will produce a series of pulse in the FrFT domain.

According to the time-shifting property of FrFT, it's easy to get the relationship between delay and pulse spacing in FRFT domain:

$$\tau_N = \Delta f_u/\cos\alpha,$$

where τ_N is the delay of paths, α is the rotation angle corresponding to the optimal order p, Δf_u is the pulse spacing in the FrFT dpmain.

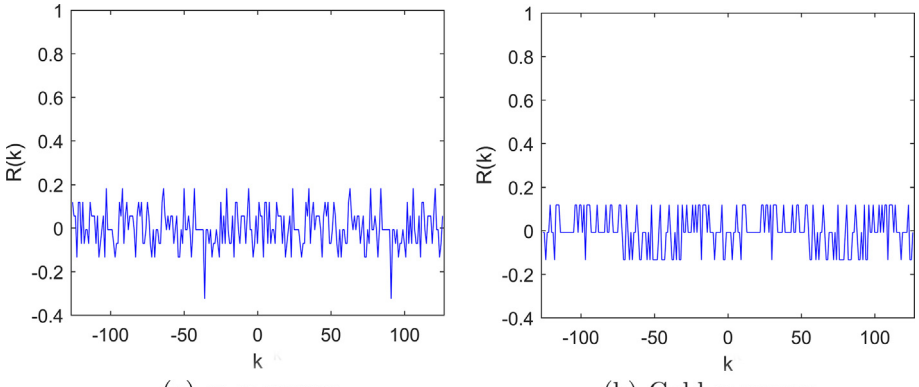

(a) m sequence. (b) Gold sequence.

Fig. 9. Cross-correlation properties of the Gold sequences and m sequences.

Fig. 10 shows a multipath channel impulse response in time domain, and Fig. 11 shows a received Chirp signal from the channel in FrFT domain.

3.3.2. Virtual time reversal mirror (VTRM)

After channel estimation, using the channel impulse response, VTRM can process the received signal and effectively resist multipath in the channel. The schematic diagram is shown in Fig. 12. Performing convolutions on received signal and channel impulse response, we can realize a time reversal mirror virtually.

VTRM introduces some noise interference that is suitable for the case of a low SNR. The processing effect depends on the accuracy of the channel estimation. After going through VTRM, the received useful signal can be expressed as:

$$r(t) = S_r(t) \otimes h'(-t) = S(t) \otimes h(t) \otimes h'(-t) + n(t) \otimes h'(-t), \tag{28}$$

where $h(t)$ is the actual channel impulse response,$h'(t)$ is the estimated channel, and $h'(-t)$ is the time reversal of the estimated channel. Let $\widehat{h}(t) = h(t) \otimes h'(-t)$,when $h'(t)$ is close to $h(t)$, $\widehat{h}(t)$ is close to the autocorrelation operation of $h(t)$. When $h(t)$ becomes more complicated, then $\widehat{h}(t)$ is closer to $\delta(t)$, which means $r(t)$ is closer to $S(t)$.

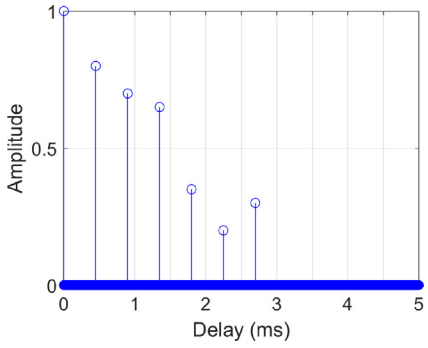

Fig. 10. CSI in time domain.

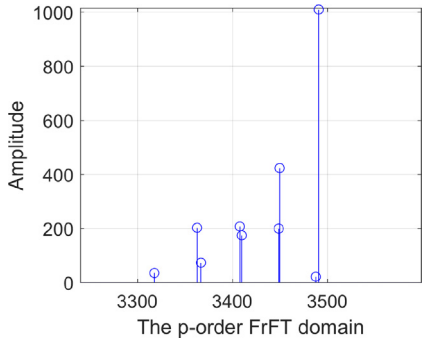

Fig. 11. Received signal in FRFT domain.

3.3.3. Demodulation and separation of multiple users

The transmission signals of several communication nodes reach the receiving end through the channel, and the received signals of the receiving end are superimposed by the M user signals. After synchronous acquisition, the received signal is given by:

$$S_r(t) = \sum_{m=1}^{M} C_m(t) \otimes h_m(t) + n(t), \tag{29}$$

where $C_m(t)$ represents the transmission signal of the mth user, $h_m(t)$ represents the impulse response of the subchannel from the mth user to the receiver.

After the receiver completes the synchronization acquisition of the mth user's signal, it's needed to separate the transmission signal of mth user from other users' signals, so as to correctly demodulate and obtain bit data sent by the mth user.

According to Eq. 13, due to the different Chirp-rates of different users, the optimal FrFT transform order is different. Based on the energy focusing feature of the Chirp signal in the FrFT domain, which has been shown in Fig. 3, the receiver performs FrFT transformation on the received signal corresponding to the optimal order of different users, and users' signals can be separated according to the occurrence of the peak.

Further, since the positions of the peaks of the Up-Chirp and Down-Chirp signals of the same user in the FrFT domain are different, whether the current received signal is Up-Chirp or Down-Chirp may be determined according to the position of the peak, and then the received PN code can be judged.

In summary, multi-user separation and Chirp-BOK demodulation can be performed simultaneously using the FrFT transform of the optimal order corresponding to different users.

Let the number of communication nodes be 4, and Fig. 13 shows the FrFT of the 4-users superimposed signal, where the center frequencies of the Chirp signals are all 20 kHz, the chip width is 5 ms, the Chirp-rate is 2000 kHz/s, 1500 kHz/s, 1000 kHz/s, 500 kHz/s, and the sampling rate is 100 kHz. The FrFT order is the optimal order corresponding to the 1st user.

Fig. 13 shows that under the optimal FrFT order of the user 1, only the signal of the user 1 exhibits the energy focusing property in the FrFT domain, and the signals of other users have no spikes, thereby the user 1's signal is separated from other users' signals. As shown in Fig. 13a, when the received signal of the user 1 is an Up-Chirp, the position where the peak appears is on the right side of the FrFT domain, and conversely, as shown in Fig. 13b, when the received signal is a Down-Chirp, the peak position is on the left side of the FrFT domain. Based on this, the determination of the received PN code can be done, the Chirp-BOK demodulation is completed. Finally, the user 1's PN sequence is used to despread the signal, and the user 1's bit data can be obtained.

4. Performance analysis

This section focuses on the anti-noise and multi-path performance of the FrFT demodulation in the communication system.

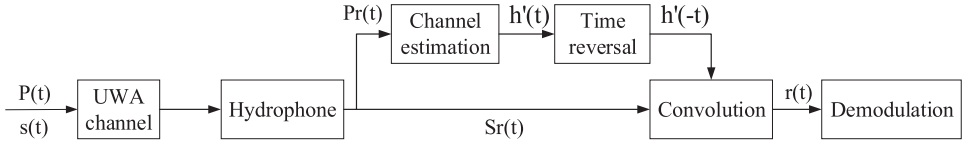

Fig. 12. Block diagram of VTRM.

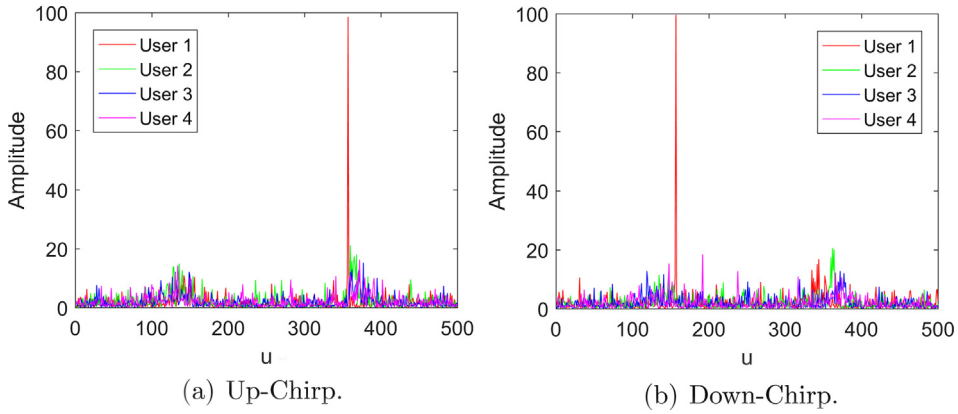

Fig. 13. The FrFT waveform of received signal (SNR $= -5dB$).

4.1. Anti-noise performance

Assume that a discrete signal $x(k)$ is superimposed with a random noise, thus the peaks in the FrFT domain appear random fluctuations and have a certain mean square error (MSE).

$$\frac{\mathcal{V}\left(|X_{p_0}(u_0)+N_{p_0}(u_0)|^2\right)}{|X_{p_0}(u_0)|^2}=\frac{2|A_{\alpha_0}|^2A^2}{(2F)^2\mathrm{SNR}_{\mathrm{in}}^2}+\frac{2|A_{\alpha_0}|^2A^2}{(2F)^2\mathrm{SNR}_{\mathrm{in}}}(2N+1), \quad (30)$$

where $\mathcal{V}(\cdot)$ denotes the variance, $N_{p_0}(u_0)$ is the noise amplitude at the signal peaks, N is the data length, the input $\mathrm{SNR}_{\mathrm{in}}=A^2/(\sigma_n^2)$, F is the maximum frequency of the signal, $A_{\alpha_0}=\sqrt{1-j\cot\alpha_0}$, and k is a coefficient adjusted depending on the actual situation. It can be seen that when the sampling rate and parameters of the signal are determined, the $\mathrm{SNR}_{\mathrm{in}}$ become an important factor affecting the relationship between the peaks.

We set an attenuation parameter m based on the relative fluctuation of the peaks, and it's given by:

$$m=k\sqrt{\frac{2|A_{\alpha_0}|^2A^2}{(2F)^2\mathrm{SNR}_{\mathrm{in}}^2}+\frac{2|A_{\alpha_0}|^2A^2}{(2F)^2\mathrm{SNR}_{\mathrm{in}}}(2N+1)}, \quad (31)$$

Set the $F=30$ kHz, $N=10,000$, $k=1$, $A=1$, and $A_{\alpha_0}=\sqrt{1-j}$, the relation between SNR and the threshold m is shown in Fig. 14. It can be seen that the larger the SNR, the smaller the peak attenuation of the Chirp signal in the FrFT domain. Overall, even with a SNR of $-10dB$, the peak attenuation coefficient is still below 0.02, which indicates that at low SNR conditions, the peak fluctuation caused by noise has a very limited effect on peak detection. Unless the noise is too strong, the waveform in the FrFT domain fluctuates too much, and the peak cannot be detected correctly, otherwise the demodulation method using FrFT can still obtain good performance at low SNR. (See Fig. 15).

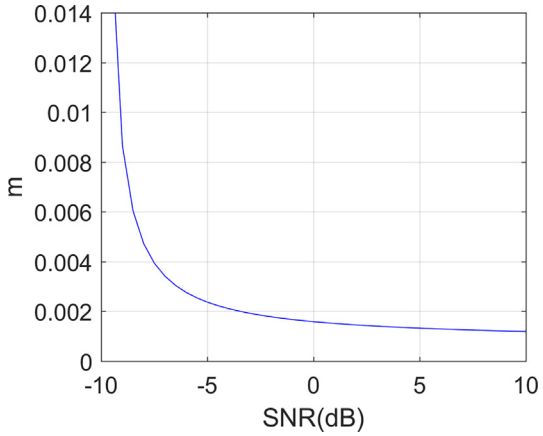

Fig. 14. Relation between SNR and amplitude attenuation.

4.2. Anti-multipath performance

The FRFT of the Chirp signal is very sensitive to time delay. When the signal reaches the receiving end through the non-direct path, compared with the signal from the direct path, there will be a certain degree of time delay. When the FrFT transform is used to process the received signal of the direct path, the impact of non-direct path signals to the system can be effectively reduced. Take a Chirp signal as an example, and it's given by:

$$f(t)=A\exp(j2\pi f_0t+j\pi\mu t^2+j\phi), T\in[-T/2,T/2]. \quad (32)$$

When there is no time delay, FrFT transforms the signal in $[-T/2,T/2]$, and let the $\mu=-\cot(\alpha)$ and $f_0=u\csc(\alpha)$, where u is the position of the peak in the FrFT domain. Then the value of the peak is given by:

$$|F_\alpha(u)|^2|_{\mu=-\cot\alpha,f_0=u\csc\alpha}=\frac{A^2T^2}{|\sin\alpha|}. \quad (33)$$

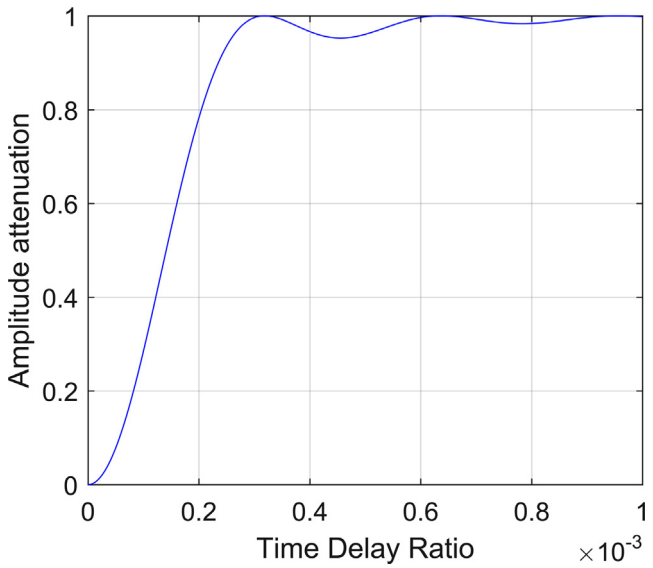

Fig. 15. Relation between delay ratio and amplitude attenuation.

When there is a time delay τ, the range of the LFM signal for the FrFT transformation is considered as $[-T/2+\tau, T/2]$. Then, the value of the peak is given by:

$$|F_\alpha(u)|^2|_{\mu=-\cot\alpha, f_0=u\csc\alpha} = \frac{A^2(T-|\tau|)^2}{|\sin\alpha|}\mathrm{sinc}^2(\pi\mu\tau(T-|\tau|)). \quad (34)$$

The attenuation coefficient is obtained by the subtraction of Eq. (33) and Eq. (34):

$$\theta = 1-(1-|\eta|)^2\mathrm{sinc}^2\left(\pi\mu T^2\eta(1-|\eta|)\right), \quad (35)$$

where η is the delay ratio, and $\eta = \tau/T$.

Fig. 14 shows the relation between delay ratio and amplitude attenuation, where the bandwidth $B = 10kHz$, and $T = 0.1s$. It can be seen that as the delay ratio increases, the amplitude of the peak in the FrFT domain decays very quickly. That is to say, due to the sensitivity of the amplitude attenuation, the Chirp signal received from the non-direct path has a large attenuation in the FrFT domain. Although the received signal of the non-direct path also forms a peak in the FrFT domain, these peaks after attenuation are difficult to affect the peak detection of the signal from the direct path, which means the system can still have good performance under the multipath channel.

5. Simulation and experiment analysis

Fig. 16 shows the flow chart of the simulation and experiment. The bit data of each user is firstly spread using corresponding PN sequence and then modulated using Chirp-BOK. In order to better simulate the underwater node positioning system, each user's transmitted signal passes through the subchannel separately, and noise and random time delay are added to the signals. The receiver synchronizes the signals of users, and performs channel estimation and VTRM processing, separately, and then performs FrFT for demodulation. Finally, the PN sequences are used to despread the data, and the bit data sent by each user is obtained.

5.1. Simulation over AWGN channel

In order to verify the anti-noise performance of the proposed multiple access communication system, the simulation is performed here under the AWGN channel, To reflect the anti-noise and anti-multipath performance of the Chirp signal, the FH-CDMA system is used here as a comparison. The FH-CDMA system modulates the signal by a single-frequency carrier of a hopping frequency controlled by PN sequences, thereby spread the spectrum of the transmitted signal and realizing broadband communication.

The parameters of the simulation are set as follows: the sampling frequency f_s of the system is 100 kHz, the frequency band used by the system is 20 kHz–30 kHz, the chip width of the Chirp signal is 10 ms, and the 8-bit Gold sequences are used. According to Section 3.2, Chirp carriers are allocated to different numbers of users. When the number of users is 4, the parameters of simulation can be seen in Table 1.

Fig. 17 shows the FrFT of the received signal under different SNRs, where the number of users is 4, and the FrFT order here is the optimal order of the user 1. When the Eb/N0 is $10dB$, in the FrFT domain, the low SNR has a limited effect on the peak amplitude of the Chirp signal, and the value at the peak does not change much. However, the fluctuation of the FrFT waveform caused by noise is very large, and it is very likely that the peak of the Chirp signal cannot be detected correctly. When Eb/N0 is increased to 15 dB, the waveform fluctuation caused by noise cannot affect the correct detection of the Chirp signal's peak, so the BER is greatly reduced (shown in Fig. 18).

Fig. 18 shows the BER of the two systems at different Eb/N0 (dB). It can be seen that when the Eb/No is lower than 10 dB, the BER of the two systems are relatively high, and normal communication cannot be achieved. However, when the Eb/No is higher than 10 dB, the BER of the proposed method is greatly reduced, although the performance of the FH-CDMA system also improves with the increase of the Eb/No, but when the BER is on the order of 10^{-4}, the performance of the proposed method is about 3 dB higher than that of the FH-CDMA system. In addition, the performance of the system drops by about 1 dB when the number of

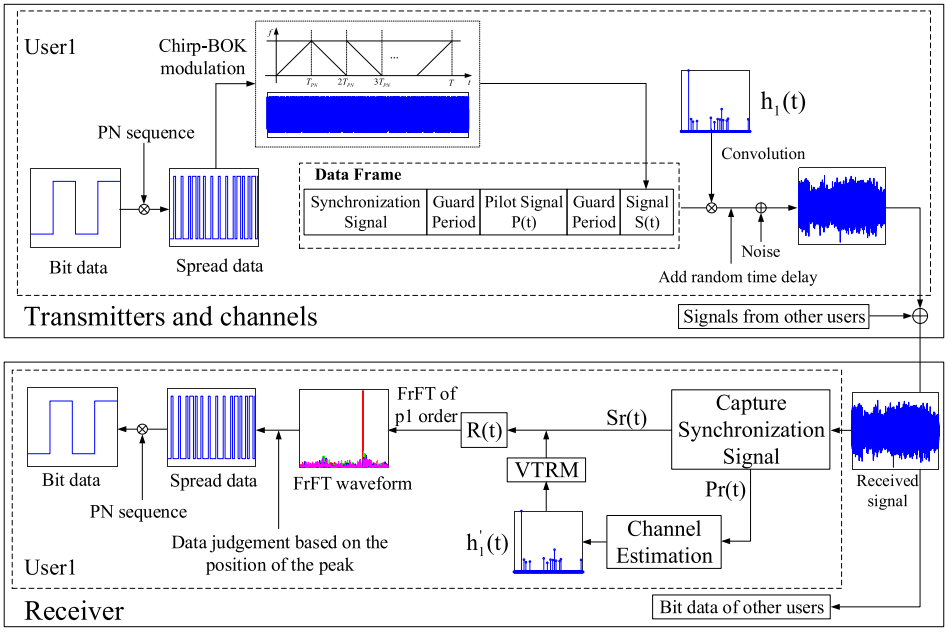

Fig. 16. Framework of simulation.

Table 1
The parameters of Chirp signals and PN sequences of 4 users.

User	Chirp signal				Gold
	Frequency range	Bandwith	Chip width	Chirp-rate	sequence
user1	20–30 [kHz]	10 [kHz]	0.01 [s]	1000 [kHz/s]	ρ_1
user2	20–27.5 [kHz]	7.5 [kHz]		750 [kHz/s]	ρ_2
user3	20–25 [kHz]	5 [kHz]		500 [kHz/s]	ρ_3
user4	20–22.5 [kHz]	2.5 [kHz]		250 [kHz/s]	ρ_4

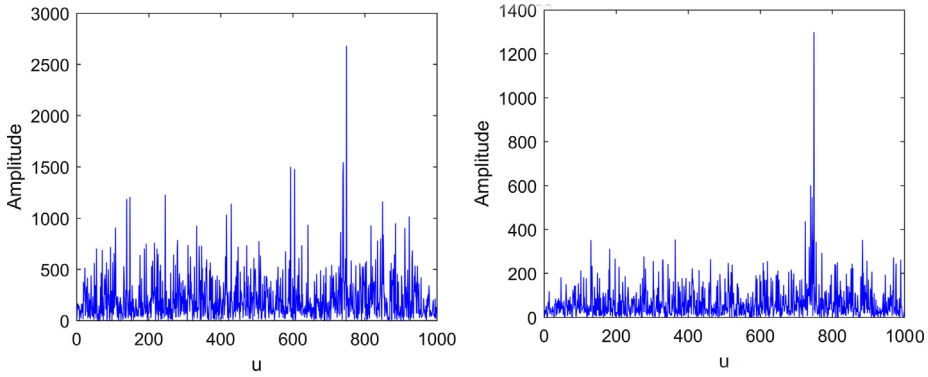

(a) Eb/N0 = 10 dB. (b) Eb/N0 = 15 dB.

Fig. 17. The FrFT waveform of received signal (Up-Chirp).

users change from 3 to 4, and when the number of users increases to 5, the BER performance of the system is greatly reduced, but still better than that of FH-CDMA. This is because the Δk decreases as the number of users increases, and the correlation coefficient ρ between the Chirp signals rises, which lead to the increase of MAI.

5.2. Simulation over multipath channel

In order to verify the anti-multipath performance of the proposed system, Bellhop model [27] is used to generate the multipath channel for simulation. The parameters of UWA channel are listed in Table 2. The bandwidth occupied by the system is from 20 kHz to 30 kHz. The chipwidth of the Chirp signals is 10 ms, and the sampling rate is 100 kHz.

Table 2
The parameters of the simulation channel using the Bellhop model.

Parameter	value
Communication distance	1000 [m]
Depth of transducer	10 [m]
Depth of receiver transducer	15 [m]
Root mean square of surface roughness	2 [m]
Acoustic velocity	1530 [m/s]
Absorption coefficient of longitudinal wave	0.5
Depth of water	20 [m]
Seawater density	1021 [kg/m^3]
Silt density	1810 [kg/m^3]
Number of transmit beams	6

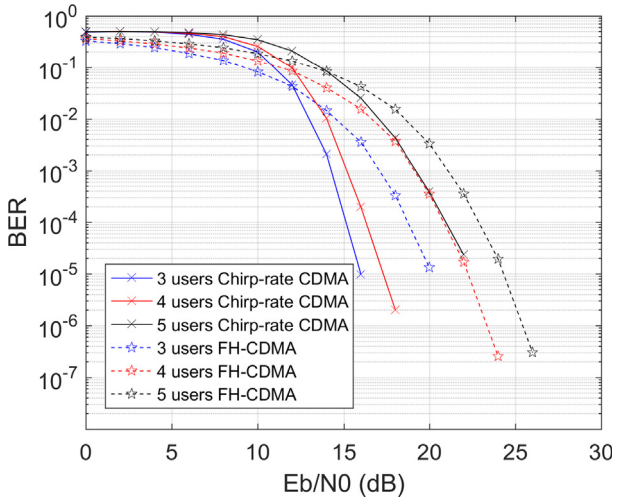

Fig. 18. BER performance under AWGN channel.

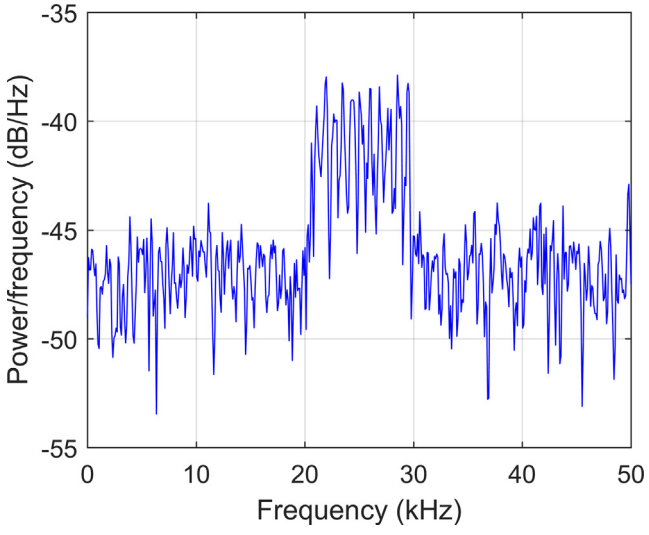

Fig. 19. PSD of the received signal.

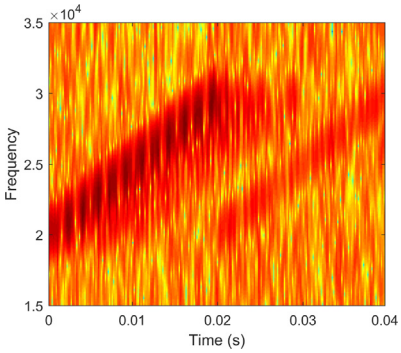

Fig. 20. Time-frequency relation.

Fig. 19 and Fig. 20 respectively show the power spectral density (PSD) and time-frequency relation of the received pilot Chirp signal from the Bellhop channel. Fig. 19 shows that in multipath channels, frequency selective fading occurs. We can see the multipath component of the received pilot signal from Fig. 20, wherein the delay of the latest multipath in the Bellhop channel is about 20 ms.

Fig. 21 shows the FrFT waveform of the received signal at different SNRs. Compared with Fig. 17, it can be seen that under the interference of noise, channel estimation and VTRM cannot completely eliminate multipath effects, so peaks of multipath components still appear in the FrFT domain, which leads to a drop of the BER performance compare with that under the AWGN channel. However, according to the analysis in Section 4.2, the multipath component is attenuated severely in the FrFT domain, so the system performance is still good with the improvement of the SNR.

Fig. 22 shows the BER performance. It can be seen that the performance of the two schemes is affected to varying degrees. FH-CDMA uses a frequency-hopped single-frequency carrier, which is very sensitive to the frequency selective fading. Under the multipath channel, the performance of FH-CDMA system is very poor. Due to the excellent anti-multipath feature of the Chirp signal, the BER performance of the proposed system can still ensure reliable communication. Compared with the performance under AWGN channel, when the BER is on the order of 10^{-4}, the performance is reduced by about 3 dB (3 users).

To more intuitively demonstrate the performance of the system, a 4-users access system was simulated. Among them, user 1 and user 2 respectively send two different pictures, and the transmission data of other users are random bits.

Figs. 23 and 24 show the comparison of the transmitted and received pictures of the two users at different Eb/N0. When the Eb/N0 is 15 dB, the BER of user 1 is very low, but the BER of the user

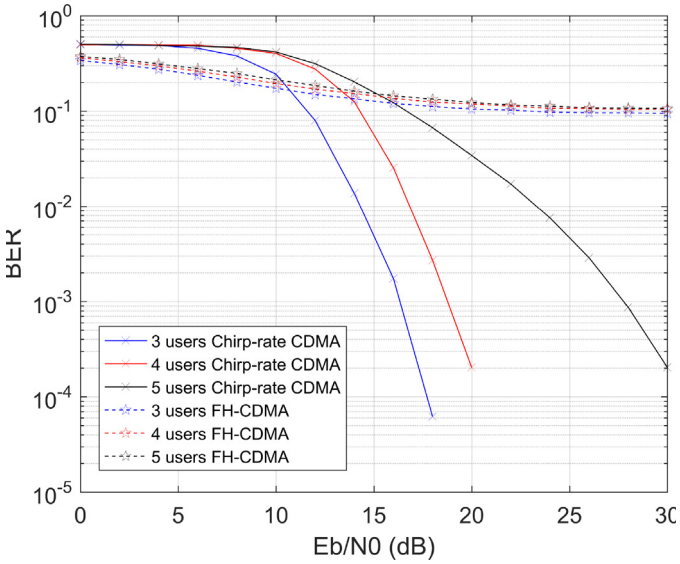

Fig. 22. BER performance under Bellhop multipath channel.

2 is on the order of 10^{-2}. This is because the Chirp signal used by user 2 has less BT than that of user 1, which reduces the anti-noise and anti-multipath performance. When the Eb/N0 is 20 dB, the BERs of both users reach zero, however, the overall BER of the system is 4.840×10^{-4}, which indicates that users 3 and 4 have error bits, and the result further confirms the above analysis.

5.3. Pool experiment

In order to further verify the applicability of the proposed system, a pool experiment was carried out to simulate the positioning system of the pool. The experimental data confirms the effectiveness of the proposed system.

Fig. 25 shows the experimental pool scenario, where there are two senders, at a depth of 70 cm from the water surface, are used to simulate the anchor nodes in the positioning system.

Since there are only two access users, in order to minimize the MAI and ensure the communication quality of each user, the resource allocation of the two users here is shown in Table 3. The time bandwidth product actually occupied by the two users are 100 and 50, respectively, and the correlation coefficient ρ of the Chirp carriers is close to zero.

Fig. 26a and Fig. 26b respectively show the channel impulse response of the two transmitters to the receiver. As can be seen,

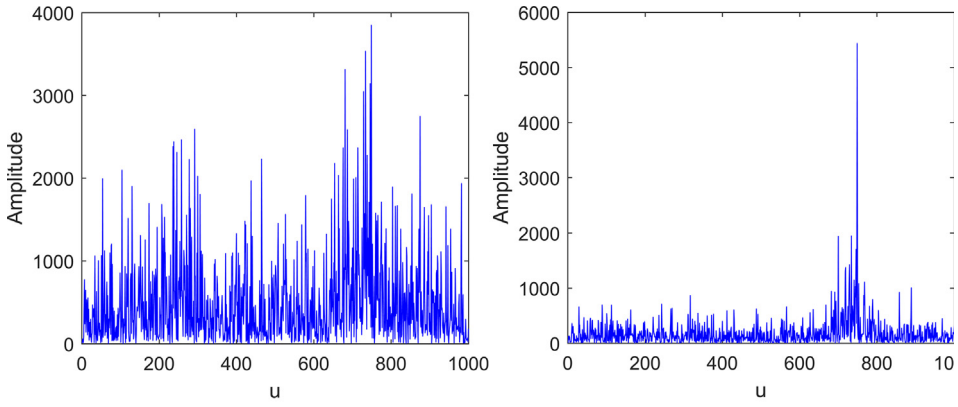

(a) Eb/N0 = 10 dB. (b) Eb/N0 = 15 dB.

Fig. 21. The 1st user's FrFT waveform of received signal (Up-Chirp).

(a) Original image. (b) Eb/N0 = 15dB, BER = 0.042%. (c) Eb/N0 = 20dB, BER = 0.

Fig. 23. Original and received images of user 1.

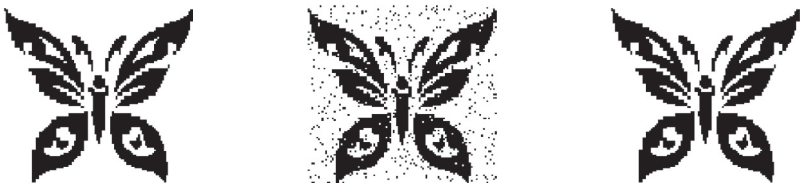

(a) Original image. (b) Eb/N0 = 15dB, BER = 3.998%. (c) Eb/N0 = 20dB, BER = 0.

Fig. 24. Original and received images of user 2.

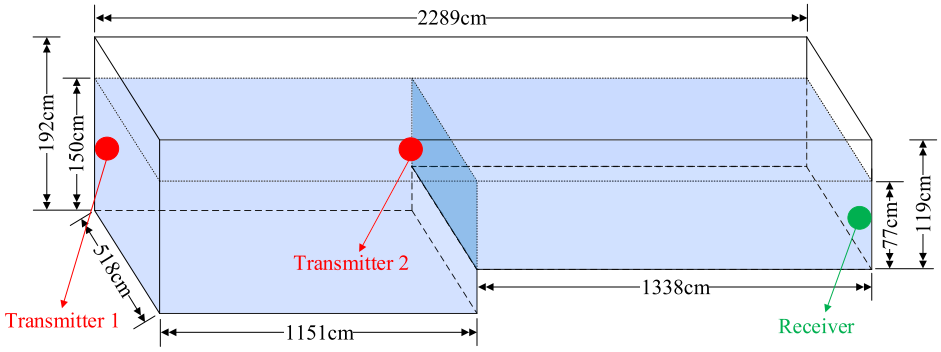

Fig. 25. Pool structure.

the multipath structure in the pool channel is very complicated. The side, bottom and water surfaces of the pool reflect the signal multiple times.

Fig. 27a shows the spectrum of the received signal, while Fig. 27b shows the time-frequency relation and the waveform in the time domain of the received signal. It can be seen that the signals of the two users overlap in the spectrum and have different arrival times, which further creates uncertainty in the demodulation of the signal. From the waveform in the time domain, we can see that the SNR of the reveived signal is relatively high.

Two transmitters simultaneously send different pictures to the receiver, which have been shown in Fig. 23a and Fig. 24a. Fig. 28 shows the received images. As can be seen, even if the multipath of the pool channel is very complicated, and the arrival time of the two user signals is different, the BER of the two users reach zero, which confirms the effectiveness of the proposed system in practical applications.

6. Conclusion

In this paper, a Chirp carrier-based CDMA multiple access system is proposed for the communication collision problem of different positioning nodes in underwater node location. Firstly, according to the quasi-orthogonality between signals of different Chirp-rates, Chirp carriers are allocated to different anchor nodes, and the allocation of different PN sequences is used to further suppress the MAI. Secondly, the received signals are processed by using FrFT. It can simultaneously perform multi-user separation and data demodulation. Thirdly, using the FrFT-based channel estimation method and time-reversing mirror processing of the received signal can further improve the performance of the system under multipath channels. Compared with the FH-CDMA system using single-frequency carrier with hopping frequency, the simulation results show that the proposed system has better performance under multipath channel. The results of the pool experiment further validate the practical feasibility and reliability of the proposed system.

However, due to the different Chirp-rates, the actual *BT* values occupied by users are different, and thus have different anti-noise and anti-multipath performance. According to Fig. 23b and Fig. 24b, the less the *BT* is, the worse the BER performance is. The proposed system is mainly applied to the underwater node positioning system in a certain area, which does not require too high transmission rate but requires better BER performance. Therefore, according to the actual situation, the chip width of the Chirp signal or the bandwidth occupied by the whole system can be increased,

Table 3
Parameters of the signals in experiment.

User	Chip width	B	Chirp-rate	Δk	ρ
user1	0.01 [s]	10 [kHz]	1000 [kHz/s]	500 [kHz/s]	0.04905
user2		5 [kHz]	500 [kHz/s]		

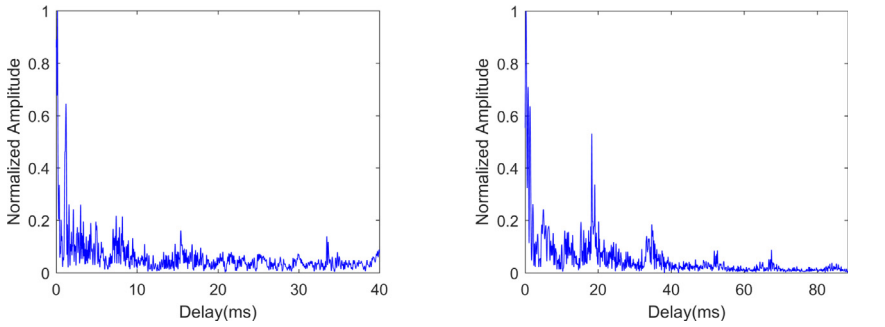

(a) Transmitter 1 to the Receiver. (b) Transmitter 2 to the Receiver.

Fig. 26. Channel impulse response of two users.

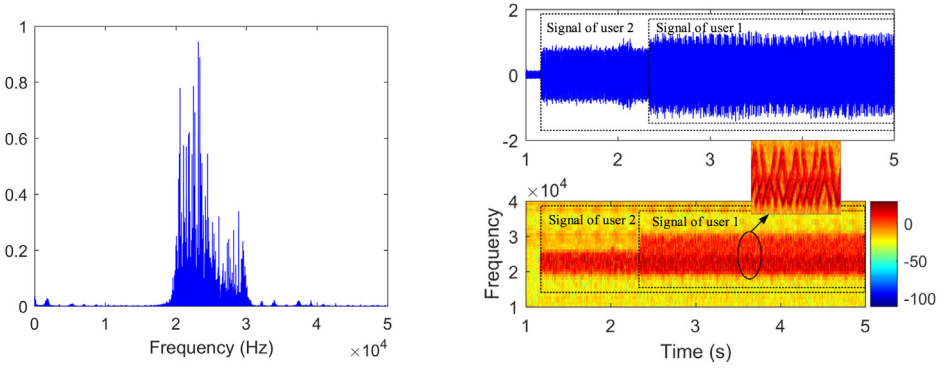

(a) Spectrum. (b) Waveform in the time domain and time-frequency relation.

Fig. 27. Received signal.

(a) user 1, BER = 0. (b) user 2, BER = 0.

Fig. 28. Received images.

so that the *BT* occupied by a single user can be increased, thereby improving the BER performance of each user, and at the same time enhancing the quasi-orthogonality between Chirp signals, further improving the overall reliability of the system.

In the simulation, the Doppler effect is not introduced. Due to the movement of the node to be located, a certain degree of Doppler effect is caused. Chirp signal also have good anti-Doppler performance due to the spread spectrum characteristics. In fact, the main factors affecting the performance of the proposed system are fluctuations in the FrFT waveform caused by high noise and an increase in MAI caused by excessive user access. In the underwater node positioning system, when the number of anchor nodes is 3, the position information of the node to be located can be obtained. Morever, Chirp-BOK modulation and FrFT demodulation are easy to implement on hardware and have a low amount of computation, which makes it possible to apply the proposed system to an actual underwater node positioning system.

References

[1] Cheng W, Teymorian AY, Ma L, Cheng X, Lu X, Lu Z. Underwater localization in sparse 3d acoustic sensor networks. In: INFOCOM 2008. the Conference on Computer Communications. IEEE; 2008. p. 236–40.
[2] Akyildiz IF, Pompili D, Melodia T. Underwater acoustic sensor networks: research challenges. Ad Hoc Netw 2005;3(3):257–79.
[3] Chitre M, Shahabudeen S, Stojanovic M. Underwater acoustic communications and networking: recent advances and future challenges. Mar Technol Soc J 2008;42(1):103–16.
[4] Pickholtz RL, Schilling DL, Milstein LB. Theory of spread-spectrum communications–a tutorial. IEEE Trans Commun 1982;30(5):855–84.
[5] Kaplan ED. Understanding gps: principles and application. J Atmos Solar Terr Phys 1996;59(5):598–9.

[6] Zhang G, Hovem JM, Dong H, Zhou S, Du S. An efficient spread spectrum pulse position modulation scheme for point-to-point underwater acoustic communication. Appl Acoust 2010;71(1):11–6.
[7] He C, Huang J, Zhang Q, Yan Z. Study on m-ary spread spectrum underwater acoustic communication. China Ordnance 2008;4(1):26–9.
[8] Zhou Y, Cao X, Yanyi WU, Tong F. Spread spectrum underwater acoustic communication based on passive time reversal in time varying channels. Appl Acoust 2015;34(6):509–15.
[9] Du P, Han X, Yin J, Zhang X. Experimental demonstration of underwater acoustic communication using bionic signals. Appl Acoust 2014;78(4):7–10.
[10] Tsai YR, Chang JF. The feasibility of combating multipath interference by chirp spread spectrum techniques over rayleigh and rician fading channels. In: IEEE ISSSTA 1994. IEEE Third International Symposium on Spread Spectrum Techniques and Applications, vol. 1, 1994, pp. 282–286..
[11] Wang X, Fei M, Li X. Performance of chirp spread spectrum in wireless communication systems. IEEE Singapore International Conference on Communication Systems 2009:466–9.
[12] Cook CE. Linear fm signal formats for beacon and communication systems. IEEE Trans Aeros Electron Syst AES-10 1974(4):471–8.
[13] Hengstler S, Kasilingam DP, Costa AH. A novel chirp modulation spread spectrum technique for multiple access, in: IEEE Seventh International Symposium on Spread Spectrum Techniques and Applications, vol. 1, 2002, pp. 73–77..
[14] Ju Y, Barkat B. A new efficient chirp modulation technique for multi-user access communications systems. In: IEEE International Conference on Acoustics, Speech, and Signal Processing, 2004. Proceedings, vol. 4; 2004, pp. iv–937–40..
[15] Meng F, Gu X. A combined chirp signal modulation technique for multiple access system. Inf Technol J 2011;10(2):416–21.
[16] Sha XJ, Wen RH, Qiu X. A new multiple-access method based on fractional fourier transform. In: Canadian Conference on Electrical and Computer Engineering. CCECE '09, 2009, pp. 856–859..
[17] Kocian A, Dahlhaus D. Downlink performance analysis of a cdma mobile radio system with chirp modulation. Vehicular Technology Conference, IEEE 1999;1:238–42.
[18] El-Khamy S, Shaaban SE, Thabet EA. Frequency-hopped multi-user chirp modulation (fh/m-cm) for multipath fading channels. Radio Science Conference. NRSC'99 1999:C6/1–8.
[19] Gupta C, Papandreou-Suppappola A. Wireless cdma communications using time-varying signals. In: International, Symposium on Signal Processing & Its Applications, vol. 1; 2001, pp. 242–245..
[20] He P, Lv Y, Zhang H, Wang Y, Xu Y. Saw chirp fourier transform for mb-ofdm uwb receiver. J China Univ Posts Telecommun 2006;13(3):1–4.
[21] Correal NS, Swanchara SF, Woerner BD. Implementation issues for multiuser ds-cdma receivers. Int J Wireless Inf Networks 1998;5(3):257–79.
[22] Mitchell OH. Digital computation of the fractional fourier transform. IEEE Trans Signal Process 1996;44(9):2141–50.
[23] Ruhang W, Jianguo H, Tian M, Qunfei Z. Improved space time prewhitener for linear frequency modulation reverberation using fractional fourier transform. J Acoust Soc Am 2010;128(6):EL361.
[24] Chen Y, Guo L, Gong Z. The concise fractional fourier transform and its application in detection and parameter estimation of the linear frequency-modulated signal. Chin J Acoust 2017;36(1):70–86.
[25] Yuan F, Wei Q, Cheng E. Joint virtual time reversal communications with an orthogonal chirp spread spectrum over underwater acoustic channel. Appl Acoust 2017;117:122–31.
[26] Zhang Xinyu. Analysis of m-sequence and gold-sequence in cdma system. In: IEEE 3rd International Conference on Communication Software and Networks. ICCSN. p. 466–8.
[27] Porter MB. The bellhop manual and user's guide: Preliminary draft, Heat, Light, and Sound Research Inc, La Jolla, CA, USA, Tech. Rep..